Revista Ciência Agronômica, v. 52, n. 4, e20207565, 2021
Centro de Ciências Agrárias - Universidade Federal do Ceará, Fortaleza, CE
www.ccarevista.ufc.br

Scientific Article
ISSN 1806-6690

Poultry by-products as source of collagen, nanokeratin and bioapatite for biomedical use[1]

Subprodutos avícolas como fonte de colágeno, nanoqueratina e bioapatita para uso biomédico

Francisco Fábio Pereira de Souza[2], Fabio Lima Cavalcante[3], Igor Iuco Castro-Silva[4]*, André Luis Coelho da Silva[5], Men de Sá Moreira de Souza Filho[6]

ABSTRACT - Xenogeneic sources are attractive for the development of natural and sustainable biomaterials. The objective of this study was to extract and perform the physicochemical and biological characterization of poultry collagen (G1), nanokeratin (G2) and bioapatite (G3). The test materials were analyzed through SEM, FTIR, TGA, EDS and DRX. The *in vivo* biocompatibility and biodegradation of the materials were analyzed histopathologically in mice at 1, 3 and 9 weeks post-subcutaneous grafting compared to positive (collagen or commercial bone) and negative (no graft) controls. The obtained data was submitted to intergroup statistical analysis using the ANOVA method with the Tukey-Kramer post-hoc test, and differences were considered significant for $p < 0.05$. G1 had an irregular filamentous microstructure typical of type I collagen, a band spectrum of amide A, I, II and III, common to proteins and compatible with triple helix maintenance, and mass loss after 40.5 °C. G2 had blades of various sizes with rough surface, with bands of amide I, II and reduced amide A and mass loss after 50 °C. G3 presented as white powder, free of organic matter, Ca/P ratio of 1.54, bands of type A and B carbonate substitution, high crystallinity and mass loss after 150 °C. All groups exhibited biocompatibility, with a non-irritating pattern in G1 and slight irritation in G2 and G3, while biodegradation was complete in G1 and G2 and partial in G3. The observed biomimicry, biocompatibility and biodegradation suggest the potential of poultry collagen and nanokeratin as hemostatic agents and bioapatite for bone grafting, requiring future orthotopic efficacy studies.

Key words: Keratins. Durapatite. Materials testing. Biocompatible materials.

RESUMO - Fontes xenógenas são atrativas para o desenvolvimento de biomateriais naturais e sustentáveis. Este estudo objetivou a extração e a caracterização físico-química e biológica de colágeno (G1), nanoqueratina (G2) e bioapatita (G3) avícolas. Os materiais-teste foram analisados por MEV, FTIR, TGA, EDS e DRX. Biocompatibilidade e biodegradação *in vivo* dos materiais foram analisadas histopatologicamente em camundongos em 1, 3 e 9 semanas pós-enxertia subcutânea em comparação aos controles positivos (colágeno ou osso comercial) e negativo (sem enxerto). Os dados obtidos foram submetidos à análise estatística intergrupos pelo método de ANOVA com pós-teste de Tukey-Kramer, sendo consideradas diferenças significativas se $p < 0,05$. G1 apresentou microestrutura filamentosa irregular típica do colágeno tipo I, espectro de bandas de amidas A, I, II e III comuns a proteínas e compatíveis com manutenção da tripla hélice e perda de massa a partir de 40,5 °C. G2 apresentou lâminas de diversos tamanhos com superfície rugosa, com bandas de amida I, II e reduzida amida A e perda de massa a partir de 50 °C. G3 apresentou pó branco, livres de matéria orgânica, relação Ca/P de 1,54, bandas de substituição por carbonato tipo A e B, alta cristalinidade e perda de massa a partir de 150 °C. Todos os grupos exibiram biocompatibilidade, com padrão não irritante em G1 e pouco irritante em G2 e G3, enquanto a biodegradação foi total em G1 e G2 e parcial em G3. Biomimetismo, biocompatibilidade e biodegradação observados indicam potencial de colágeno e nanoqueratina avícolas para agentes hemostáticos e de bioapatita para enxerto ósseo, sendo necessários futuros estudos ortotópicos de eficácia.

Palavras-chave: Queratinas. Durapatita. Teste de materiais. Materiais biocompatíveis.

DOI: 10.5935/1806-6690.20210049
Editor-in-Chief: Prof. Alek Sandro Dutra - alekdutra@ufc.br
*Author for correspondence
Received for publication 15/08/2020; approved on 14/01/2021
[1]Trabalho extraído das dissertações do primeiro autor, apresentada ao Programa de Pós-graduação em Biotecnologia da Universidade Federal do Ceará (UFC) Campus de Sobral, e do segundo autor, apresentada ao Programa de Pós-graduação em Química (UFC) Campus de Fortaleza
[2]Departamento de Engenharia de Pesca, Programa de Pós-graduação em Biotecnologia de Recursos Naturais, Universidade Federal do Ceará (UFC), Fortaleza-CE, fabiosouzawin@gmail.com (ORCID ID 0000-0002-3086-7954)
[3]Departamento de Físico-Química e Analítica, Programa de Pós-graduação em Química, Universidade Federal do Ceará (UFC), Fortaleza-CE, fabiolima2008@hotmail.com (ORCID ID 0000-0002-5247-0667)
[4]Laboratório de Biomateriais, Programa de Pós-graduação em Biotecnologia, Universidade Federal do Ceará (UFC), Sobral-CE, igor.iuco@sobral.ufc.br (ORCID ID 0000-0003-4815-6357)
[5]Departamento de Bioquímica e Biologia Molecular, Universidade Federal do Ceará, Fortaleza-CE, andre.coelho@ufc.br (ORCID ID 000-0003-0685-6398)
[6]Embrapa Agroindústria Tropical, Fortaleza-CE, men.souza@embrapa.br (ORCID ID 0000-0003-4404-2360)

INTRODUCTION

Brazil ranks second in the world in the production of poultry protein, with an output of 13 million tons of chicken meat annually, equivalent to the sum of all national production of beef, pork, and fish (CASTRO-SILVA *et al*., 2018). The global poultry industry also generates a significant amount of waste, including feathers, feet, skin, heads, and bones (ARANBERRI *et al*., 2017). An annual production of 65 billion tons is estimated for feathers alone (ZHAO *et al*., 2012).

According to the current concept for green industries, it is important to seek appropriate strategies for the disposal or reuse of processed materials to minimize environmental impacts, fostering sustainability and social responsibility (ARANBERRI *et al*., 2017; REDDY, 2015). Poultry by-products are sources of proteins, such as collagen and keratin, and minerals, such as apatite, and the study of their potential for the development of biotechnological inputs has started in the last decade (SUPOVÁ; MARTYNKOVÁ; SUCHARDA, 2011; REDDY, 2015; WANG *et al*., 2016).

Collagen is found in abundance in the skin, while keratin can be isolated from hair, nails, horns, wool, and feathers. Both are fibrous proteins that show similarity across animal species, cell adhesion and proliferation, as well as biocompatibility *in vivo* (YAO *et al*., 2017). Early preclinical studies have shown that avian collagen and keratin contribute to tissue repair, either as hemostatic or skin wound healing agents (REDDY, 2015; WANG *et al*., 2016).

Poultry bioapatite mimics human bone and would be a low cost and high availability alternative for obtaining the mineral bone fraction (SUPOVÁ; MARTYNKOVÁ; SUCHARDA, 2011). In general, natural xenogeneic apatites have a similar structure to human hydroxyapatite, with biocompatibility, bioactivity and potential applications in orthopedic and dental surgeries (ESMAEILKHANIAN *et al*., 2019).

The use of organic and inorganic avian matrices, alone or in hybrid form, in guided clinical bone regeneration procedures would represent a technological innovation. Due to their wide availability and low surgical morbidity compared to autogenous materials, these xenogeneic biomaterials would converge with the principle of sustainability and would be attractive for the development of bone substitute products (CASTRO-SILVA *et al*., 2018).

The objective of this study was to extract collagen, nanokeratin, and bioapatite from poultry industry by-products and perform a preliminarily evaluation *in vivo* of their physicochemical and biological properties for future biomedical applications.

MATERIAL AND METHODS

Sample acquisition and processing

This work was previously registered in the National System for the Management of Genetic Heritage and Associated Traditional Knowledge (*Sistema Nacional de Gestão do Patrimônio Genético e do Conhecimento Tradicional Associado* - SisGen) under registration number A576649. All raw materials from *Gallus gallus domesticus* were derived from the broiler processing waste of a poultry industry in Fortaleza, Brazil.

The collagen extraction followed an adaptation of the protocol by Zeng *et al*. (2009). 800 g of chicken skin and tendons, sanitized with hypochlorite, were treated with NaOH 0.05 mol/L 1:10 (w/v) to remove non collagenous proteins, with ethanol 10% (v/v) 1:10 (w/v) to remove lipids, and with EDTA 0.05 mol/L at pH 8 1:10 (w/v) for demineralization; all treatments were performed at 8 ºC under stirring for 24 h and interspersed with washes with distilled water for neutralization. The material was then treated with 0.5 mol/L 1:25 (v/v) of acetic acid at 8 ºC under stirring for 72 h, filtered in TNT to remove non-solubilized particles, and placed to precipitate in 0.9 mol/L of NaCl for 24 h. The precipitated collagen was centrifuged at 13,000 rpm for 5 min at 4 ºC, redissolved in 0.5 mol/L acetic acid, and subjected to a new cycle of precipitation and centrifugation as described above. Finally, the obtained collagen was dialyzed against a solution of NaHPO4-0.02 mol/L at 8 ºC for 48 h in 12-14 KDa membranes and against distilled water until neutral pH, after which it was freeze-dried and ground in an analytical impact grinding mill (Model A11BS32, IKA, Germany).

The keratin extraction followed the protocol by Saravanan *et al*. (2013). Chicken feathers previously sanitized with a neutral detergent solution were washed with 70% (v/v) alcohol to remove lipids, dried at room temperature and ground in a knife mill (Tecnal-TE 058). 100 g of ground feathers were treated with NaOH 5% (m/m) 1:40 (w/v) at 40 ºC under stirring for 4 h, filtered in TNT to remove insoluble particles, and dialyzed against distilled water for 48 h with water exchange every 24 h. The dialyzed material was precipitated through the addition of 2 mol/L-1 HCl until pH 4.2, centrifuged at 10,000 rpm for 10 min at 25 °C, neutralized in washes with distilled water, and lyophilized. To obtain the nanokeratin, 1 g of freeze-dried keratin was solubilized in 20 mL of deionized water at pH 8. Then, 80 mL of absolute ethanol was added to the solution under stirring at the rate of 1 mL/min and 10 µL of 8% (v/v) glutaraldehyde and kept under stirring for 24 h for the formation of nanoparticles. The formed nanokeratin was separated by centrifugation at 13,000 rpm for 15 min, submitted to several washing cycles in deionized water interspersed

by 5 min ultrasonication cycles until complete removal of the glutaraldehyde and, finally, lyophilized.

Hydroxyapatite extraction followed the alkaline hydrothermal method of Supová, Martynková and Sucharda (2011). 200 g of chicken foot bones were immersed in 2% (w/v) 1:10 (w/v) NaCl solution and autoclaved at 120 °C for 30 min. The material was ground in an analytical impact grinding mill (Model A11BS32, IKA, Germany), treated with an acetone:ether (3:2) 1:2 (w/v) solution for 24 h to remove lipids, and with NaOH 4% (w/v) 1:20 (w/v) for 24 h to remove proteins, and neutralized in washes with deionized water. After chemical treatment, the material was calcined in a muffle furnace at 500 °C for 18 h, washed with deionized water and dried in an oven at 80 ºC.

Physicochemical characterization

Samples of poultry collagen, nanokeratin and biopatite were characterized by Scanning Electron Microscopy (SEM), Fourier Transform Infrared Spectroscopy (FTIR) and Thermogravimetry (TGA). For the SEM analysis, the samples were gold metallized and analyzed under a ZEISS-DSM 940-A microscope at 15 kV. The FTIR analysis was performed in a FTLA 2000-102 device (ABB-BOMEM), and the TGA analysis in a STA 6000/8000 device (PerkinElmer) in a synthetic air atmosphere with a flow rate of 40 mL/min, heating rate of 10 °C/min and temperature range of 20 to 800 °C. Additionally, the bioapatite was characterized by Energy Dispersive Spectroscopy (EDS) to quantify the Ca/P molar ratio, and by X-ray diffraction (XRD) to identify crystalline materials.

***In Vivo* Biological Characterization**

The preparation of the samples for grafting was based on ISO 10993-6 (INTERNATIONAL ORGANIZATION FOR STANDARDIZATION, 2016), defining the standard relative surface area of 10 mm^2 to arrive at the individual amount of product to be inserted. The equivalent amounts of each group were weighed, arranged in plastic microtubes and sterilized by ultraviolet light for 30 min.

All procedures for animal experimentation were approved by the institutional Animal Use Ethics Committee (*Comissão de Ética no Uso de Animais*, CEUA UFC-Sobral) under protocol number 04/17. Forty-five adult, heterogeneous Swiss mice (*Mus musculus*) of both sexes and weighing 30 g were subjected to general anesthesia by intramuscular application of 100 mg/kg of ketamine (Dopalen®, CEVA, Brazil) and 12 mg/kg of xylazine (Anasedan®, CEVA, Brazil). The trunk-dorsal region was trichotomized and degermed with 0.5% alcoholic chlorhexidine (Rioquimica, São José do Rio Preto, SP, Brazil), with linear incisions of 1cm in length and delicate divulsion of the subcutaneous tissue in order to create two subdermal pockets of 10 mm^2. The test groups were collagen (G1), nanokeratin (G2) and avian bioapatite (G3). The controls were: commercial bovine collagen (Lumina Coat Double Time, Criteria, SP, Brazil), used as positive control (C_1+) for G1 and G2, bovine mineral bone (Lumina Bone, Criteria, SP, Brazil), used as positive control (C_2+) for G3, and surgical wound with blood clot and no graft, used as negative control (C-) for all groups. Each animal received a test and control group graft. Euthanasia was performed by anesthetic overdose 1, 3 or 9 weeks after surgery, with 5 animals per experimental condition.

The excisional necropsies of the grafted region were fixed for 48 h in 4% formalin (VETEC, Duque de Caxias, RJ, Brazil) buffered at pH 7.2. G3 and C_2+ were also decalcified for 1 h in a solution of 10% aqueous nitric acid and 4% buffered formalin (1:1) and washed in tap water for 1 h. The samples were then cleaved and underwent histological processing and microtomy. Sections of 5 μm were stained with the Hematoxylin-Eosin (HE) technique. All histological slides were photodocumented on a FWL-1000 optical microscope (Feldman Wild Leitz, Manaus, AM, Brazil) coupled with a Cybershot DSC-W300 Super Steady Shoot camera (Sony, Tokyo, Japan), capturing 5 non-overlapping field images at 400x magnification for each slide. They were evaluated descriptively and quantitatively under the supervision of a pathologist. The biocompatibility and biodegradation pattern for each type of graft was determined by the presence gradations ranging from 0 to 4 based on ISO 10993-6 (INTERNATIONAL ORGANIZATION FOR STANDARDIZATION, 2016) and by comparing the mean scores obtained in each experimental condition of the test groups against the controls.

For the biocompatibility analysis, the irritation pattern for each experimental condition (25 results, considering quintuplicates of animals and images for each test or control group) used three equations: (1) inflammatory pattern equation (*Ix*); (2) repair pattern equation (*Rx*); (3) general irritation pattern equation (*IP*), described below.

$$Ix = 2\Sigma\ (N + L + M + GC) \quad (1)$$

Where Ix = inflammation pattern; sub-index x = test or control group; N = mean neutrophils; L = mean lymphocytes; M = mean macrophages; GC = mean giant cells.

$$Rx = 2\Sigma\ (NV + CT) \quad (2)$$

Where Rx = repair pattern; sub-index x = test or control group; NV = mean neovascularization; CT = mean connective tissue.

$$IP = (I_t + R_t) - (I_{c-} + R_{c-}) \quad (3)$$

Where IP = Irritation pattern; I_t = test group inflammation pattern; R_t = test group repair pattern; I_{c-} = negative control inflammation pattern; R_{c-} = negative control repair pattern.

The ISO 10993-6 (INTERNATIONAL ORGANIZATION FOR STANDARDIZATIONS, 2016) standard defines biocompatibility standards for grafted materials, including: non-irritating (0-2.9), slightly irritating (3-8.9), moderately irritating (9-15) or severely irritating (> 15). In case of a negative result by subtraction of negative control, the irritation standard is considered zero.

For the biodegradability analysis, the morphological integrity of the grafts in subcutaneous tissue over the experimental times was calculated using increasing presence gradations of the material in quartiles, ranging from 0 (absent), 1 (< 25%), 2 (< 50%), 3 (< 75%) to 4 (> 75%). The average pattern for each test group per experimental condition (25 results, considering quintuplicates of animals and images for each group) was compared to its respective positive control.

The GraphPad InStat software, version 3.0 (GraphPad Software, Inc., USA), was used for the statistical analysis of the distribution of mean values ± standard deviations of the biocompatibility and biodegradability in order to compare test and control groups. The One-Way ANOVA with the Tukey-Kramer post-hoc test was adopted, and differences were considered significant if $p < 0.05$.

RESULTS AND DISCUSSION

Physicochemical Analysis of the Samples

Figure 1 shows the macro and microscopic structure of poultry collagen (G1), nanokeratin (G2) and bioapatite (G3). G1 showed an irregular filamentous microstructure typical of type I collagen and a clean-looking surface, free of non-collagenous proteins or inorganic material (Figure 1), which qualitatively confirms the efficiency of the removal processes of these constituents in the samples. These findings are characteristic of type I collagen samples, indicative of a high-water absorption potential (ZENG *et al*., 2009). G2 showed blades of various sizes with a rough surface, a thickness of approximately 200 nm and a mean nanoparticle size of 167 nm, obtained as weighted mean (Figure 1). Saravanan *et al*. (2013) obtained keratin nanoparticles in a similar process with a spherical morphology. This suggests that the laminar aspect of the obtained nanokeratin may be the result of aggregation resulting from the freeze-drying process. G3 presented as a white powder with fine granulometry, evidence of the removal of organic constituents in the bone (Figure 1).

The EDS spectrum showed a typical composition of biological apatites, being composed mostly of Ca and P and other minority elements (C, O, Mg, Br and Na), usually

Figure 1 - Macroscopy (**A**) and SEM (**B**) of poultry collagen, nanokeratin and bioapatite

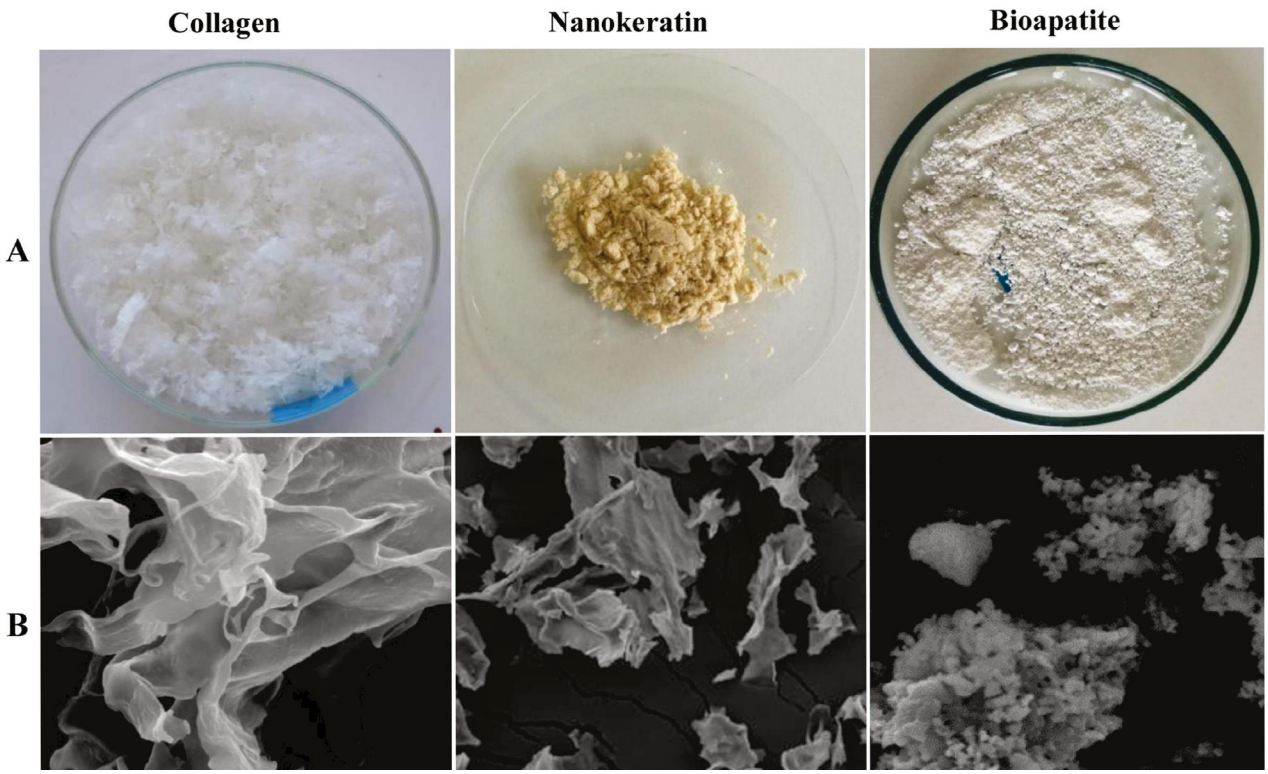

accepted as resulting from the substitutions they occupy in the crystal structure. The Ca/P molar ratio of G3 was 1.54 ± 0.06. This value is lower than the 1.67 of stoichiometric hydroxyapatite (HA) and close to the 1.63-1.64 of other calcium-deficient biological apatites derived from poultry through the alkaline hydrothermal method, and it is indicative of potential bioactivity and biocompatibility (ESMAEILKHANIAN *et al*., 2019; ŠUPOVÁ; MARTYNKOVÁ; SUCHARDA, 2011).

Figure 2 shows the chemical composition and thermal stability results of test groups G1, G2, and G3. G1 had a spectrum of Amide A bands at 3300 cm^{-1} associated with the vibrational stretching of N-H bonds, presenting a shift from 3400 to 3300 cm^{-1}, related to the existence of hydrogen bonds between the chains; Amide I at 1628 cm^{-1} referring to the vibrational stretching of carboxylic groups; Amide II at 1550 cm^{-1} related to the angular deformation of the N-H bond; Amide III at 1238 cm^{-1} associated with the vibrational increase of C-N bonds; and the band at 1452 cm^{-1}, associated with the deformation of C-H groups of the pyrrolidine ring of the proline and hydroxyproline, bands related to the integrity of the triple helix (Figure 2A). Mass loss or denaturation occurred after 40.5 °C (Figure 2B). Both the triple helix maintenance and the denaturation temperature are in line with reports in the literature for collagen obtained from chicken skins and extracted in acid solution (SANTANA *et al*., 2020; ZENG *et al*., 2009). G2 showed a band at 1538 cm^{-1} characteristic of the N-H bending of proteins (Amide II); a band at 1632 cm^{-1} related to the vibrational stretching of C=O bonds of the amide groups and particularly sensitive to the secondary structure of proteins, representing a slight shift of Amide I, which may be a result of the amplification of zones with a β configuration, since keratin also presents minority portions of α-helix configuration (ZHAO *et al*., 2012); and a decreased band at 3300 cm^{-1} (Amide A) (Figure 2A), related to the presence of ordered α-helix regions and symmetric N-H bond stretching (YAO *et al*., 2017). Such a decrease may also be related to the way in which glutaraldehyde crosslinks, which, according to the literature, occurs mainly through the formation of shiff bases with the amino groups of the proteins. As a result, the availability of these groups is reduced (REDDY, 2015). Even with crosslinking, mass loss occurred after 50 °C and reached 80% (Figure 2B), being associated with the breaking of disulfide bonds, breaking of peptide bonds and degradation of the protein structure, a similar behavior to other poultry keratin (ARANBERRI *et al*., 2017). G3 did not show bands referring to organic matter present in the bone *in natura*, but it had bands at 870 cm^{-1} referring to the presence of carbonate as type B substitution (when part of the $PO4^{3-}$ groups are replaced by CO_3^{2-} in the crystal structure) and at 878 cm^{-1} (Figure 2A), slightly smaller and referring to type A carbonate substitution (when OH groups are replaced by carbonate). Still, the carbonate content was equivalent to 5.02%. The mass loss between 150 °C and 310 °C was progressive, equivalent to 0.5% of mass, suggesting some remaining organic aggregate, increasing to 2.5% after 310 °C (Figure 2B).

The X-ray diffraction analysis showed narrow and well-defined peaks (Figure 3), revealing a high degree of correlation with the characteristic peaks of hydroxyapatite present in the PDF-2-ICDD-01-082-1943 datasheet, which is compatible with high crystallinity.

Figure 2 - FTIR (**A**) and TGA (**B**) of poultry collagen, nanokeratin and bioapatite

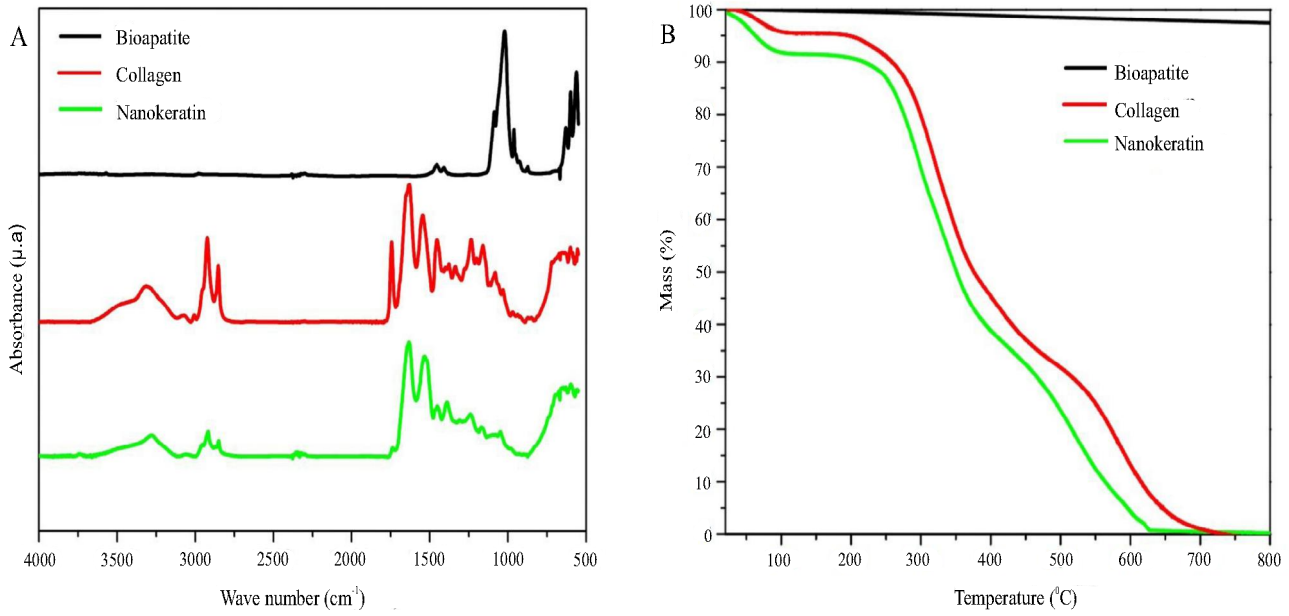

Based on the diffractograms, a 95% crystallinity index was also quantified. The absence of organic matter confirms the complete removal of organic constituents after calcination (RAMESH *et al*., 2018). The hardness of apatites from bovine and goat bones is closer to that of the human cortical bone, while chicken bones exhibit phase instability with traces of βTCP (RAMESH *et al*., 2018). Nevertheless, the carbonate content of poultry bone close to human levels and the high crystallinity suggest potential for bioactivity and biocompatibility (ŠUPOVÁ; MARTYNKOVÁ; SUCHARDA, 2011). The literature reports that B-type substitution is generally predominant in biological apatite (RAMESH *et al*., 2018). Carbonate substitution in apatite is causally related to the increase in solubility, being more easily absorbed by living cells compared to pure HA, which enhances the bioactivity of bioapatites (ESMAEILKHANIAN *et al*., 2019). The carbonate content found in this bioapatite exceeds the 3.11% found in another study with chicken femur bone (ŠUPOVÁ; MARTYNKOVÁ; SUCHARDA, 2011). The mass loss accentuated by temperature may be related to the decomposition of part of the carbonate percentage present in the bioapatite. However, a high initial degradation temperature is in alignment with a decrease in the degradation rate *in vivo*, which may be determinant for applications in which the longevity of the biomaterial in the biological system is desired (RAMESH *et al*., 2018).

Figure 3 - Diffractogram of poultry bioapatite

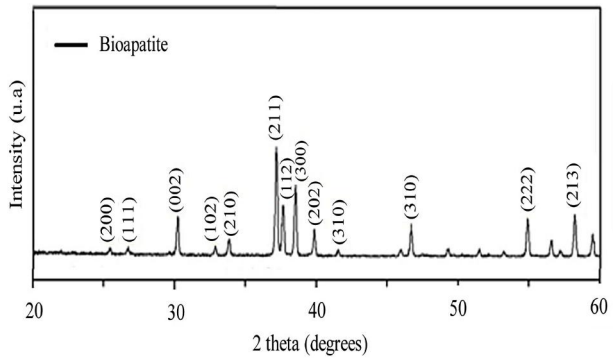

Biocompatibility analysis

Figure 4 shows distinct profiles of biological responses in mice according to time and treatment. G1 exhibited mixed inflammatory infiltrate at 1 week, well-vascularized granulation tissue at 3 weeks, and loose connective tissue with areas of fibrosis at 9 weeks. G2 exhibited mixed inflammatory infiltrate at 1 week, granulation tissue rich in multinucleated foreign body giant cells at 3 weeks, and the persistence of granulation tissue at 9 weeks. These phenomena were like C_1+, with mixed inflammatory infiltrate at 1 week, granulation tissue at 3 and 9 weeks, maintaining its stable structure until the end of the experiment. G3 showed

Figure 4 - Histopathological analysis of the biocompatibility of poultry collagen (**G1**), nanokeratin (**G2**), bioapatite (**G3**) *versus* the positive controls' commercial collagen (**C_1+**) (for G1 and G2) and commercial bone (**C_2+**) (for G3), grafted into the subcutaneous tissue of mice over the period of 1 week (**A-E**), 3 weeks (**F-J**) and 9 weeks (**K-O**). Staining: HE, Magnification: 40x. Scale bar: 200 µm. Neutrophilic (*) or lymphocytic (**) inflammatory infiltrate, multinucleated foreign body-like giant cells (►), blood vessels (→), connective tissue (**C**) and material (**M**). Staining: HE, Magnification: 400x. Scale bar: 20 µm

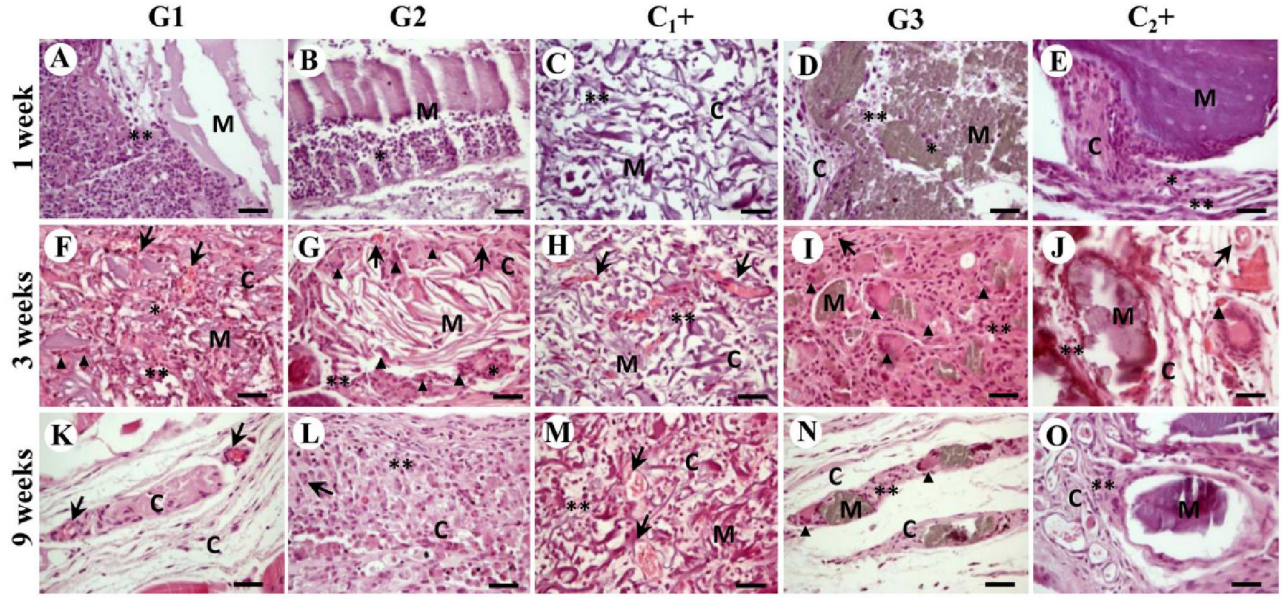

mononuclear inflammatory infiltrate at 1 week, vascularized granulation tissue with moderate presence of multinucleated foreign body giant cells at 3 weeks, and the persistence of giant cells at 9 weeks, with granulation tissue giving way to loose connective tissue or areas of fibrosis. C_2+ showed mild polymorphonuclear inflammatory infiltrate at 1 week, minimal inflammatory infiltrate at 3 and 9 weeks, with some giant cells, compatible with its partial resorption.

Table 1 shows the biocompatibility found for groups G1, G2 and the controls. Along the experimental period, there was a decrease in the irritation pattern, classified at 9 weeks as non-irritant for G1, like C_1+, and as slightly irritant for G2, which was different from the non-irritant pattern found in its respective positive controls (C_1+ and C_2+). As for the statistical differences in the biological criteria under analysis, varied profiles were observed according to time and experimental group. For G1, the presence of neutrophils and lymphocytes at 1 week and lymphocytes and macrophages at 3 weeks was higher than in C_1+ ($p < 0.001$) and C- ($p < 0.001$); neovascularization was higher than in C_1+ ($p < 0.001$) and C- ($p < 0.01$) at 1 week, while the presence of connective tissue was higher than in C_1+ ($p < 0.01$, $p < 0.001$, $p < 0.01$) at 1, 3 and 9 weeks, respectively. For G2, the presence of neutrophils at 1 week and lymphocytes at 1 and 3 weeks was superior to C_1+ ($p < 0.001$) and C- ($p < 0.001$); the presence of lymphocytes at 9 weeks was also superior to C- ($p < 0.001$); the presence of macrophages was superior to C_1+ ($p < 0.05$) at 1 week and to C_1+ ($p < 0.001$) and C- ($p < 0.001$) at 3 and 9 weeks; the presence of giant cells was higher than in C- ($p < 0.001$) at 3 weeks and C_1+ ($p < 0.05$) and C- ($p < 0.01$) at 9 weeks; neovascularization was higher than in C_1+ ($p < 0.001$) at 1 week, as was the presence of connective tissue compared to C- ($p < 0.01$) at 1 week.

Table 1 - Quantitative analysis of the biocompatibility of poultry collagen (G1) and nanokeratin (G2) *versus* controls in the subcutaneous tissue of mice over the experimental times (T) of 1, 3 and 9 weeks (w) (mean ± standard deviation of 25 fields per treatment)

Criteria		T	Experimental groups and p* values							
			G1	*p*		G2	*p*		C_1+	C-
				C_1+	*C-*		*C_1+*	*C-*		
INFLAMMATION	Neutrophils	1w	1.56 ± 1.47	*0.001*	*0.001*	2.16 ± 1.82	*0.001*	*0.001*	0.16 ± 0.62	0.24 ± 0.44
		3w	0.32 ± 0.56	-	-	0.80 ± 1.23	-	-	0.12 ± 0.33	0.08 ± 0.28
		9w	0.04 ± 0.20	-	-	0.16 ± 0.37	-	-	0	0
	Lymphocytes	1w	2.80 ± 0.41	*0.001*	*0.001*	2.60 ± 0.50	*0.001*	*0.001*	2.28 ± 0.80	0.72 ± 0.46
		3w	2.40 ± 0.65	*0.001*	*0.001*	1.92 ± 0.81	*0.001*	*0.001*	1.60 ± 1.00	0.60 ± 0.50
		9w	0.60 ± 0.50	-	-	1.32 ± 0.75	-	*0.001*	0.76 ± 0.72	0.44 ± 0.51
	Macrophages	1w	0.68 ± 0.48	-	-	0.80 ± 0.41	*0.05*	-	0.28 ± 0.46	0.40 ± 0.56
		3w	2.08 ± 1.63	*0.001*	*0.001*	1.92 ± 1.12	*0.001*	*0.001*	0.04 ± 0.20	0.40 ± 0.50
		9w	0.28 ± 0.61	-	-	1.40 ± 1.36	*0.001*	*0.001*	0	0.12 ± 0.33
	FBGC	1w	0.12 ± 0.33	-	-	0	-	-	1.20 ± 0.65	0.04 ± 0.20
		3w	0.40 ± 0.50	-	-	1.36 ± 1.08	-	*0.001*	1.84 ± 0.75	0.04 ± 0.20
		9w	0.04 ± 0.20	-	-	1.44 ± 1.26	*0.05*	*0.01*	1.32 ± 0.63	0.16 ± 0.37
REPAIR	Neovascularization	1w	2.40 ± 1.08	*0.001*	*0.01*	2.04 ± 1.27	*0.001*	-	2.00 ± 1.58	1.00 ± 0.82
		3w	1.72 ± 1.14	-	-	1.68 ± 1.28	-	-	1.20 ± 0.41	1.16 ± 0.47
		9w	1.24 ± 1.13	-	-	1.48 ± 1.09	-	-	1.40 ± 1.19	1.00 ± 0.65
	Connective tissue	1w	1.40 ± 0.58	*0.01*	-	0.96 ± 0.45	-	*0.01*	1.36 ± 0.49	1.64 ± 0.49
		3w	1.68 ± 0.80	*0.001*	-	1.36 ± 0.86	-	-	1.24 ± 0.52	1.28 ± 0.46
		9w	2.12 ± 0.44	*0.01*	-	1.48 ± 0.51	-	-	1.28 ± 0.54	1.88 ± 0.67
Irritation Pattern		1w	8.68 (SI)			8.68 (SI)			0.00 (NI)	-
		3w	9.12 (MI)			10.36 (MI)			5.00 (SI)	-
		9w	0.96 (NI)			7.28 (SI)			0.24 (NI)	-

*Statistically significant values between each test group and the control groups by experimental time through One-Way ANOVA with the Tukey-Kramer post-hoc test. Test groups: poultry collagen (**G1**) and nanokeratin **(G2)**. Positive control: commercial collagen (**C_1+**). Negative control: surgical wound without graft (**C-**). Scores: non-irritating (**NI**), slightly irritating (**SI**) or moderately irritating (**MI**). **FBGC:** Foreign body multinucleated giant cells

Table 2 shows the biocompatibility found for the G3 and control groups. For G3, the presence of neutrophils at 1 week and lymphocytes at 1 and 3 weeks was higher than in C_2+ ($p < 0.001$) and C- ($p < 0.001$); the presence of macrophages was higher than in C_2+ ($p < 0.01$) at 1 week, while the presence of giant cells was higher than in C- ($p < 0.001$) at 1, 3 and 9 weeks.

The biocompatibility of polymeric materials exhibits high heterogeneity due to the wide range of compositions and processing (BOW; ANDERSON; DHAR, 2019). Biological responses vary from persistent intense acute inflammation in alginate-capsule membrane (JARDELINO *et al.*, 2012), well-vascularized granulation tissue with small to moderate intensity of lymphocytes or presence of multinucleated giant cells in collagenous (JARDELINO *et al.*, 2010) and cellulosic biomaterials (LUZ *et al.*, 2020) to local fibrosis in polymer-ceramic composites based on PLGA, HA and βTCP (PEREIRA *et al.*, 2019) or collagen and HA (BITTENCOURT *et al.*, 2014). For bioceramics and bioglass, the presence of multinucleated giant cells or granulation tissue in the host tissue-biomaterial interface starting at 3 weeks is already expected as a chronic inflammatory response to mineralized grafts with moderate to high crystallinity (GIORNO *et al.*, 2014; LOMELINO *et al.*, 2012; SENA *et al.*, 2014). Natural collagen of xenogeneic origin (bovine or porcine) has been widely studied for its high biocompatibility and angiogenic and agglutinating capacity, and it is applicable as a framework or membrane barrier (BITTENCOURT *et al.*, 2014; JARDELINO *et al.*, 2010). Poultry collagen exhibits low immunogenicity and has

Table 2 - Quantitative analysis of the biocompatibility of poultry bioapatite (G3) *versus* controls in the subcutaneous tissue of mice over the experimental times (T) of 1, 3 and 9 weeks (w) (mean ± standard deviation of 25 fields per treatment)

Criteria		T	Experimental groups and p* values				
			G3	*p*		C_2+	C-
				C_2+	*C-*		
INFLAMMATION	Neutrophils	1w	1.56 ± 1.47	*0.001*	*0.001*	0.16 ± 0.62	0.24 ± 0.44
		3w	0.08 ± 0.28	-	-	0.12 ± 0.33	0.08 ± 0.28
		9w	0.08 ± 0.28	-	-	0	0
	Lymphocytes	1w	2.84 ± 0.37	*0.001*	*0.001*	2.28 ± 0.80	0.72 ± 0.46
		3w	2.40 ± 0.50	*0.001*	*0.001*	1.60 ± 1.00	0.60 ± 0.50
		9w	0.80 ± 0.65	-	-	0.76 ± 0.72	0.44 ± 0.51
	Macrophages	1w	1.08 ± 0.57	*0.01*	-	0.28 ± 0.46	0.40 ± 0.56
		3w	0.72 ± 0.46	-	-	0.04 ± 0.20	0.40 ± 0.50
		9w	0.24 ± 0.44	-	-	0	0.12 ± 0.33
	FBGC	1w	1.32 ± 0.90	-	*0.001*	1.20 ± 0.65	0.04 ± 0.20
		3w	2.48 ± 0.87	-	*0.001*	1.84 ± 0.75	0.04 ± 0.20
		9w	2.24 ± 0.60	-	*0.001*	1.32 ± 0.63	0.16 ± 0.37
REPAIR	Neovascularization	1w	1.24 ± 1.05	-	-	2.00 ± 1.58	1.00 ± 0.82
		3w	1.60 ± 0.87	-	-	1.20 ± 0.41	1.16 ± 0.47
		9w	1.64 ± 0.91	-	-	1.40 ± 1.19	1.00 ± 0.65
	Connective tissue	1w	1.16 ± 0.37	-	-	1.36 ± 0.49	1.64 ± 0.49
		3w	1.56 ± 0.51	-	-	1.24 ± 0.52	1.28 ± 0.46
		9w	1.76 ± 0.60	-	-	1.28 ± 0.54	1.88 ± 0.67
Irritation Pattern		1w	10.56 (MI)			5.76 (SI)	-
		3w	9.84 (MI)			4.96 (SI)	-
		9w	5.80 (SI)			2.52 (NI)	-

*Statistically significant values between each test group and the control groups by experimental time through One-Way ANOVA with the Tukey-Kramer post-hoc test. Test group: poultry bioapatite (**G3**). Positive control: commercial bone (**C_2+**). Negative control: surgical wound without graft (**C-**). Scores: non-irritating (**NI**), slightly irritating (**SI**) or moderately irritating (**MI**). **FBGC:** Foreign body multinucleated giant cells

potential clinical usability (PENG *et al*., 2010). When used as a skin covering, poultry keratin accelerates epithelial and connective repair, increasing the number of blood vessels (YAO *et al*., 2017). Natural bovine or alloplastic apatites, single (HA) or biphasic (HA-βTCP), also exhibit adequate biocompatibility (BITTENCOURT *et al*., 2014; GIORNO *et al*., 2014; LOMELINO *et al*., 2012). There is scarce evidence of the biocompatibility of poultry collagen and keratin (PENG *et al*., 2010; WANG *et al*., 2016; YAO *et al*., 2017) and a lack of subcutaneous testing with poultry apatite, which makes this validation study important for new products. Composites seem to be strategic for the development of biocompatible and biomimetic materials for application in bone tissue (BITTENCOURT *et al*., 2014) and the synergism between G1, G2 and G3 may be explored in the future.

Biodegradability Analysis

Figure 5 shows distinct integrity profiles of the grafted materials according to time and treatment. G1 and G2 suffered a decrease in their initial volume at 1 week post-grafting until they completely disappeared at 9 weeks, while C_1+ remained stable. G3 suffered a decrease in its initial volume at 1 week post-grafting until it underwent partial resorption at 9 weeks, while C_2+ remained stable.

Table 3 shows the observed biodegradability profile for the test groups compared to their respective positive control group. G1 and G2 showed lower integrity than C_1+ ($p < 0.001$) at 1 and 3 weeks, while they completely disappeared at 9 weeks. G3 showed higher integrity than C_2+ ($p < 0.001$) at 1 week and both remained present at the end of 9 weeks.

Figure 5 - Histopathological analysis of the biodegradability of poultry collagen (**G1**), nanokeratin (**G2**), bioapatite (**G3**) *versus* the positive controls' commercial collagen (**C_1+**) (for G1 and G2) and commercial bone (**C_2+**) (for G3), grafted into the subcutaneous tissue of mice along the period of 1 week (**A-E**), 3 weeks (**F-J**) and 9 weeks (**K-O**). Material (**M**). Staining: HE, Magnification: 40x. Scale bar: 200 µm

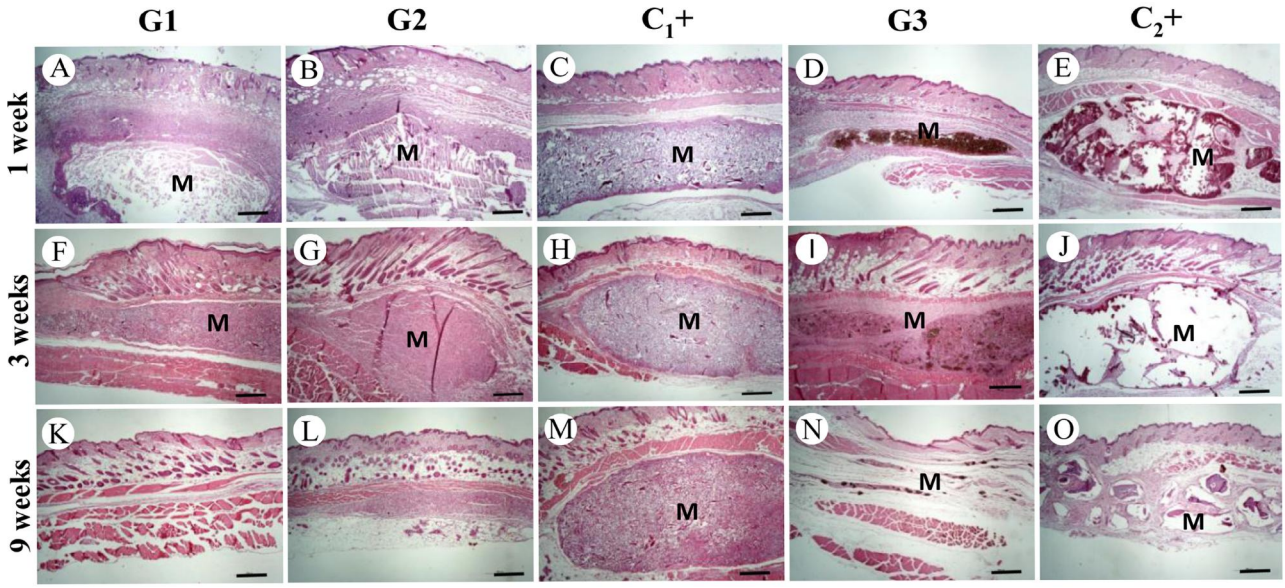

Table 3 - Quantitative analysis of graft biodegradation *versus* positive control in the subcutaneous tissue of mice over the experimental times (T) of 1, 3 and 9 weeks (w) (mean ± standard deviation of 25 fields per treatment)

Criteria	T	Experimental groups and p* values							
		G1	*p*	G2	*p*	C_1+	G3	*p*	C_2+
Integrity	1w	1.20 ± 0.71	*0.001*	0.28 ± 0.46	*0.001*	3.96 ± 0.20	3.32 ± 0.85	*0.001*	1.44 ± 0.65
	3w	0.16 ± 0.37	*0.001*	0.20 ± 0.41	*0.001*	3.88 ± 0.33	2.64 ± 0.76	-	2.48 ± 0.77
	9w	0	*0.001*	0	*0.001*	2.48 ± 1.81	1.76 ± 0.93	-	1.84 ± 0.75

*Statistically significant values between each test group and its respective positive control per experimental time by One-Way ANOVA with Tukey-Kramer post-test. Test groups: collagen (**G1**), nanokeratin (**G2**), bioapatite (**G3**). Positive controls: commercial collagen (**C_1+**) (for G1 and G2) and commercial bone (**C_2+**) (for G3)

Polymeric materials tend to have more pronounced biodegradability (JARDELINO *et al*., 2010), while bioceramics (GIORNO *et al*., 2014) and bioglasses (SENA *et al*., 2014) show good structural stability and resistance to biological degradation. Composites with chicken keratin and PLA show complete degradation (ARANBERRI *et al*., 2017), while HA and collagen remain with almost complete stability after weeks in the subcutaneous tissue of rats (BITTENCOURT *et al*., 2014). Such evidence explains the rapid degradation of G1 and G2 compared to G3. The optimal degradation rate should be compatible with tissue regeneration, varying according to the biomedical application (LUZ *et al*., 2020). From this perspective, G1 and G2 seem to be applicable as hemostatic agents, and useful as frameworks for days to weeks, whereas G3 could be developed as a bone graft to remain for weeks to months during surgical recovery.

CONCLUSIONS

Poultry collagen, nanokeratin and biopatite showed good physicochemical characteristics, including purity and structural stability, good biocompatibility and biomimicry. Collagen and nanokeratin showed a high rate of biodegradability, undergoing total resorption within 3 weeks, while bioapatite showed a low rate of biodegradability, undergoing partial resorption at the end of 9 weeks post-grafting.

ACKNOWLEDGMENTS

The authors are grateful to the Post-Graduation Programs in Biotechnology, Biotechnology of Natural Resources and Chemistry, and Central Analitica from Federal University of Ceara - UFC; Embrapa Agroindustria Tropical - Unit of Fortaleza; FUNCAP (Process BPI n. BP3-0139-00270.01.00/18), CNPq and CAPES (DS, code 001) research funding agencies. The authors are also grateful to Morsyleide de Freitas Rosa, professor of the Post-Graduation Program in Chemistry from UFC and researcher of the Embrapa, and to scientific scholarships students Lana Karine Araujo, Mateus Aragão Esmeraldo, Sarah Rodrigues Basilio, Juliana Dantas da Costa and Paula Bianca Viana Pinheiro.

REFERENCES

ARANBERRI, I, M. S *et al.* Fully biodegradable biocomposites with high chicken feather content. **Polymers**, v. 11, n. 9, e593, 2017.

BITTENCOURT, R. C. *et al.* Preclinical evaluation of a xenogenic hydroxyapatite/collagen-based bone substitute material. **Revista Odonto Ciência**, v. 29, n. 1, p. 6-13, 2014.

BOW, A.; ANDERSON, D. E.; DHAR, M. Commercially available bone graft substitutes: the impact of origin and processing on graft functionality. **Drug Metabolism Reviews**, v. 51, n. 4, p. 533-544, 2019.

CASTRO-SILVA, I. I. *et al.* Biotechnological potential of by-products of the Brazilian animal protein industry in the generation of xenogeneic biomaterials for bone regeneration. **Trends in Research**, v. 1, n. 3, p. 1-2, 2018.

ESMAEILKHANIAN, A. *et al.* Synthesis and characterization of natural nano-hydroxyapa-tite derived from turkey femur-bone waste. **Applied Biochemistry and Biotechnology**, v. 189, n. 5, p. 1-14, 2019.

GIORNO, B. *et al*. Comparative in vivo study of biocompatibility of apatites incorporated with 1% zinc or lead ions versus stoichiometric hydroxyapatite. **Journal of Biomimetics, Biomaterials and Tissue Engineering**, v. 19, p. 109-120, 2014.

INTERNATIONAL ORGANIZATION FOR STANDARDIZATION. **ISO 10993-6**-: Biological evaluation of medical devices – Part 6: Tests for local effects after implantation, Geneva, Switzerland: ISO, 2016.

JARDELINO, C. *et al*. Biocompatibility analysis of a novel reabsorbable alloplastic membrane composed of alginate-capsul. **Revista Gaúcha de Odontologia**, v. 60, n. 4, p. 419-423, 2012.

JARDELINO, C. *et al.* Porcine peritoneum as source of biocompatible collagen in mice. **Acta Cirurgica Brasileira**, v. 25, n. 4, p. 332-336, 2010.

LOMELINO, R. O. *et al.* The association of human primary bone cells with biphasic calcium phosphate (βTCP/HA 70:30) granules increases bone repair. **Journal of Materials Science-Materials in Medicine**, v. 23, n. 3, p. 781-788, 2012.

LUZ, E. P. C. G. *et al.* Resorbable bacterial cellulose membranes with strontium release for guided bone regeneration. **Materials Science & Engineering C: Materials for Biological Applications**, v. 116, e111175, 2020.

PENG, Y. Y. *et al*. Evaluation of the immunogenicity and cell compatibility of avian collagen for biomedical application. **Journal of Biomedical Materials Research Part A**, v. 93, n. 4, p. 1235-1244, 2010.

PEREIRA, L. C. *et al*. In vitro physico-chemical characterization and standardized in vivo evaluation of biocompatibility of a new synthetic membrane for guided bone regeneration. **Materials (Basel)**, v. 12, n. 7, e1186, 2019.

RAMESH, S. *et al.* Characterization of biogenic hydroxyapatite derived from animal bones for biomedical applications. **Ceramics International**, v. 44, n. 2018, p. 10525-30, 2018.

REDDY, N. Non-food industrial applications of poultry feathers. **Waste Management**, v. 45, p. 91-107, 2015.

SANTANA, J. C. C. *et al.* Valorization of chicken feet by-product of the poultry industry: high qualities of gelatin and biofilm from extraction of collagen. **Polymers (Basel)**, v. 12, n. 3, e529, 2020.

SARAVANAN, D. K. *et al*. Chitosan scaffolds containing chicken feather keratin nanoparticles for bone tissue engineering. **International Journal of Biological Macromolecules**, v. 62, p. 481-486, 2013.

SENA, L. A. *et al*. Biocompatibility of wollastonite-poly(*N*-butyl-2-cyanoacrylate) composites. **Journal of Biomedical Materials Research Part B: Applied Biomaterials**, v. 102, n. 6, p. 1121-1129, 2014.

SUPOVÁ, M.; MARTYNKOVÁ, G. S.; SUCHARDA, Z. Bioapatite made from chicken femur bone. **Ceramics–Silikáty**, v. 55, n. 3, p. 256-260, 2011.

WANG, J. *et al.* Feather keratin hydrogel for wound repair: preparation, healing effect and biocompatibility evaluation. **Colloids and Surfaces B: Biointerfaces**, v. 149, p. 341-350, 2016.

YAO, C. *et al.* Novel bilayer wound dressing based on electrospun gelatin/keratin nanofibrous mats for skin wound repair. **Materials Science and Engineering: C**, v. 79, p. 533-540, 2017.

ZENG, S. K. *et al.* Isolation and characterisation of acid-solubilised collagen from the skin of Nile tilapia (Oreochromis niloticus). **Food Chemistry**, v. 116, p. 879-883, 2009.

ZHAO, W. *et al.*, Sustainable and practical utilization of feather keratin by an innovative physicochemical pretreatment: high density steam flash-explosion. **Green Chemistry**, v. 14, n. 12, p. 3352, 2012.

This is an open-access article distributed under the terms of the Creative Commons Attribution License